the DN, and the solvent dielectric constant (ϵ), but in all three cases no good correlations were obtained. Solvents of higher donor number (HMP and py) as well as high acceptor number (NMF) were utilized, but no well-defined correlations were observed. This is similar to the case of $((CN)_4TPP)FeCl$[26] and is most likely due to the poor binding ability of the different solvents to reduced $((CN)_4TPP)Co$.

Acknowledgment. Support of the National Science Foundation (Grant No. CHE-8515411) is gratefully acknowledged. We also acknowledge helpful discussions with Dr. Madhav Chavan.

Registry No. $((CN)_4TPP)Co^{II}$, 71147-59-6; $((CN)_4TPP)Co^{II}(py)$, 103190-70-1; $((CN)_4TPP)Co^{II}(py)_2$, 103190-71-2; $[((CN)_4TPP)Co^{III}]^+$, 103190-72-3; $[((CN)_4TPP)Co^{III}(py)_2]^+$, 103200-96-0; $[((CN)_4TPP)Co^{II}]^-$, 103190-73-4; $[((CN)_4TPP)Co^{II}(py)]^-$, 103190-74-5; $[((CN)_4TPP)Co^{I}]^{2-}$, 103190-75-6; $[((CN)_4TPP)Co^{I}]^{3-}$, 103190-76-7; pyridine, 110-86-1.

Contribution from the Department of Chemistry, Purdue University, West Lafayette, Indiana 47907

Three Forms of a Copper(III) Tripeptideamide and a Comparison of Their Photochemistry

Joanna P. Hinton and Dale W. Margerum*

Received April 9, 1986

Tri-α-aminoisobutyryl amide, Aib_3a, forms three square-planar copper(III) complexes that are stable (25 °C, in the dark) in aqueous solution from pH 0 to 14, where H_{-n} refers to the number of coordinated deprotonated nitrogens:

$$Cu^{III}(H_{-2}Aib_3a)^+ \xrightleftharpoons{pK_a = 0.25} Cu^{III}(H_{-3}Aib_3a) \xrightleftharpoons{pK_a = 12.5} Cu^{III}(H_{-4}Aib_3a)^-$$

The predominant form (pH 0.25-12.5) has an amine nitrogen, two deprotonated peptide nitrogens, and a deprotonated amide nitrogen coordinated to copper(III). In strong acid the terminal amide nitrogen is protonated, and coordination to the metal is by the amide oxygen. In strong base the amine nitrogen is deprotonated and remains coordinated to copper(III). In contrast to their stability with respect to redox decomposition, these complexes show varied photochemical sensitivity upon irradiation into their ligand-to-metal charge-transfer (LMCT) bands. Coordination by an amine nitrogen and three deprotonated amide nitrogens enhances photochemical loss of copper(III) in the UV-LMCT band ($\Phi = 0.34$) relative to coordination by an amine nitrogen, two deprotonated amide nitrogens, and a carbonyl oxygen ($\Phi = 0.30$). The opposite dependence is observed upon irradiation in the visible-LMCT band, where $\Phi = 0.16$ for $Cu^{III}(H_{-3}Aib_3a)$ and $\Phi = 0.22$ for $Cu^{III}(H_{-2}Aib_3a)^+$. Deprotonation of the terminal amine nitrogen causes a dramatic reduction in the quantum yield with $\Phi \leq 0.004$ in the visible region and 0.08 in the UV region. The photodecomposition products vary for the three complexes and are wavelength-dependent. The principal peptide oxidation products from photolysis of $Cu^{III}(H_{-3}Aib_3a)$ at pH 5 and $Cu^{III}(H_{-4}Aib_3a)^-$ in 1.0 M OH^- are substituted hydantoins, which are proposed to form by a metal-assisted intramolecular nucleophilic reaction. The different photodecomposition mechanisms are discussed.

Introduction

Stabilization of trivalent copper is no longer considered unusual. A variety of donor groups have been used to coordinate copper in this high oxidation state, including deprotonated peptide nitrogens,[1-4] amidate nitrogens,[5] sulfur groups,[6-9] and macrocyclic polyamine, amide, imide, and azine nitrogens.[10-15] These copper(III) complexes have been characterized by X-ray crystallography,[4,5,7,9,11] EXAFS,[16] electrochemistry,[2,5,8,14,17] proton- and electron-transfer reactions,[18-28] and their photochemical behavior.[3,8,29]

Bis(dithiooxalato-*S*,*S*')copper(III) is reported to undergo a light-activated, intramolecular ligand-to-copper two-electron transfer with cleavage of the C-C bond in the ligand and generation of gaseous SCO.[8] Copper(III) peptides also undergo photoinduced redox decomposition upon irradiation of their lig-

(1) Margerum, D. W.; Chellappa, K. L.; Bossu, F. P.; Burce, G. L. *J. Am. Chem. Soc.* **1975**, *97*, 6894-6896.
(2) Bossu, F. P.; Chellappa, K. L.; Margerum, D. W. *J. Am. Chem. Soc.* **1977**, *99*, 2195-2203.
(3) Kirskey, S. T., Jr.; Neubecker, T. A.; Margerum, D. W. *J. Am. Chem. Soc.* **1979**, *101*, 1631-1633.
(4) Diaddario, L. L.; Robinson, W. R.; Margerum, D. W. *Inorg. Chem.* **1983**, *22*, 1021-1025.
(5) Birker, P. J. M. W. L. *Inorg. Chem.* **1977**, *16*, 2478-2482.
(6) Wijinhoven, J. G.; van den Hark, T. E. M.; Beurskers, P. T. *J. Cryst. Mol. Struct.* **1972**, *2*, 189-196.
(7) Coucouvanis, D.; Hollander, F. J.; Caffery, M. L. *Inorg. Chem.* **1976**, *15*, 1853-1860.
(8) Imamura, M. R.; Gordon, G.; Coucouvanis, D. *J. Am. Chem. Soc.* **1984**, *106*, 984-990.
(9) Kanatzidis, M. G.; Baenziger, N. C.; Coucouvanis, D. *Inorg. Chem.* **1985**, *24*, 2680-2683.
(10) Rybka, J. S.; Margerum, D. W. *Inorg. Chem.* **1981**, *20*, 1453-1458.
(11) Oliver, K. J.; Waters, T. N. *J. Chem. Soc., Chem. Commun.* **1982**, 1111-1112.
(12) Olson, D. C.; Vasilevski, J. *Inorg. Chem.* **1971**, *10*, 463-470.
(13) Sulfab, Y.; Al-shatti, N. A. *Inorg. Chem.* **1984**, *87*, L23-L24.
(14) Castellani, C. B.; Fabbrizzi, L.; Licchelli, M.; Perotti, A.; Poggi, A. *J. Chem. Soc., Chem. Commun.* **1984**, 806-808.
(15) Kimura, E.; Sakonaka, A.; Nakamoto, M. *Biochim. Biophys. Acta* **1981**, *678*, 172-179.
(16) Kennedy, W. R.; Powell, D. R.; Niederhoffer, E. C.; Teo, B.-K.; Orme-Johnson, W. H.; Margerum, D. W., to be submitted for publication.
(17) Youngblood, M. P.; Margerum, D. W. *Inorg. Chem.* **1980**, *19*, 3068-3072.
(18) Rybka, J. S.; Kurtz, J. L.; Neubecker, T. A.; Margerum, D. W. *Inorg. Chem.* **1980**, *19*, 2791-2796.
(19) Neubecker, T. A.; Kirksey, S. T., Jr.; Chellappa, K. L.; Margerum, D. W. *Inorg. Chem.* **1979**, *18*, 444-448.
(20) Owens, G. D.; Chellappa, K. L.; Margerum, D. W. *Inorg. Chem.* **1979**, *18*, 960-966.
(21) DeKorte, J. M.; Owens, G. D.; Margerum, D. W. *Inorg. Chem.* **1979**, *18*, 1538-1542.
(22) Lappin, A. G.; Youngblood, M. P.; Margerum, D. W. *Inorg. Chem.* **1980**, *19*, 407-413.
(23) Koval, C. A.; Margerum, D. W. *Inorg. Chem.* **1981**, *20*, 2311-2318.
(24) Anast, J. M.; Margerum, D. W. *Inorg. Chem.* **1982**, *21*, 3494-3501.
(25) Anast, J. M.; Hamburg, A. W.; Margerum, D. W. *Inorg. Chem.* **1983**, *22*, 2139-2145.
(26) Owens, G. D.; Phillips, D. A.; Czarnecki, J. J.; Raycheba, J. M. T.; Margerum, D. W. *Inorg. Chem.* **1984**, *23*, 1345-1353.
(27) Dennis, C. R.; Nemeth, M. T.; Kumar, K.; Margerum, D. W., to be submitted for publication.
(28) Kumar, K.; Rotzinger, F. P.; Endicott, J. F. *J. Am. Chem. Soc.* **1983**, *105*, 7064-7074.
(29) Hamburg, A. W.; Margerum, D. W. *Inorg. Chem.* **1983**, *22*, 3884-3893.

0020-1669/86/1325-3248$01.50/0

and-to-metal charge-transfer (LMCT) bands.[3,29] The products of the photodecomposition are copper(II) in 100% yield and the original peptide in 50% yield (based on the initial amount of copper(III)). The remaining 50% of the parent peptide ligand is oxidized and recovered as peptide fragments, acetone, carbon dioxide, and ammonia. The copper(III) disappearance quantum yield as well as the identity and relative proportions of the peptide fragments are found to depend on the LMCT band irradiated. Furthermore, the photochemical behavior is found to be sensitive to the number of α-carbon methyl substituents on the peptide and the peptide length.

In the present work, the effect of different coordinated groups on the photochemical stability of copper(III) peptides is examined without changing the number of α-carbon methyl groups and the length of the peptide. This is possible with the copper(III) complexes of tri-α-aminoisobutyryl amide, Aib_3a. Three different stable forms of copper(III)–Aib_3a exist, each of which exhibits a different photoreactivity in aqueous solution. The principal form, $Cu^{III}(H_{-3}Aib_3a)$ (**1**), where H_{-3} refers to the number of coordinated

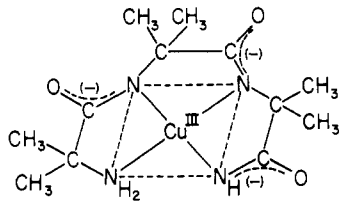

1

deprotonated nitrogens, exhibits the greatest dark stability of all the copper(III) peptides studied to date in this laboratory. Less than 3% loss of copper(III) is observed in 1 month. This stability is related to its low Cu(III/II) reduction potential of 0.37 V (NHE),[25] which is attributed to coordination by three deprotonated amide nitrogens and the electron-donating properties of the α-carbon methyl groups. For comparison, the copper(III) complex of the tripeptide, $Cu^{III}(H_{-2}Aib_3)$ (**2**), where a carboxylate oxygen

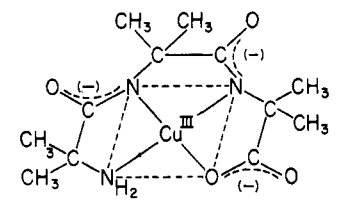

2

replaces the terminal deprotonated amide nitrogen (i.e., with only two deprotonated amide nitrogens coordinated), has a reduction potential of 0.66 V.[3] The two other forms of copper(III)–Aib_3a exist under fairly extreme conditions. In high acid the complex is $Cu^{III}(H_{-2}Aib_3a)^+$ (**3**), in which the copper(III) is coordinated by an amine nitrogen, two deprotonated peptide nitrogens, and the carbonyl oxygen of the terminal amide function. In high base $Cu^{III}(H_{-4}Aib_3a)^-$ (**4**) forms, where coordination is via three deprotonated amide nitrogens and a deprotonated amine nitrogen. The quantum yield for loss of copper(III), the photodecomposition products with their relative proportions, and the photochemical mechanisms are reported for these three different copper(III)–Aib_3a complexes.

Experimental Section

Reagents. Tri-α-aminoisobutyryl amide (Aib_3a) and the other Aib peptides (Aib_3, Aib_2a, Aib_2, and Aiba) were synthesized by A. W. Hamburg or H. D. Lee using the methods described previously.[3,30] Copper(II) perchlorate was prepared from reagent grade $CuCO_3$, and $HClO_4$ was standardized by EDTA/murexide titration.

The copper(III) complex $Cu^{III}(H_{-3}Aib_3a)$ was prepared by oxidation of a solution of the copper(II) peptide at pH 10.5 in an electrochemical bulk flow cell.[31] Typical yields were ≥95%. The pH of the eluent was between 5 and 7. 5,5-Dimethylhydantoin (**5**) was obtained from Aldrich

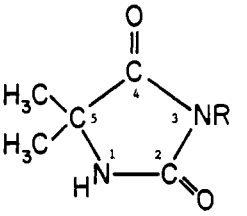

5, R = H
6, R = $C(CH_3)_2CO_2H$
7, R = $C(CH_3)_2CONH_2$

and used without further purification.

Due to the light sensitivity of the copper(III) complexes, they were handled under a Kodak 1A darkroom lamp.

Photolysis Experiments. For quantum yield determinations argon-saturated solutions were photolyzed at 25 °C with the continuous photolysis apparatus described previously.[29] The loss of copper(III) was monitored spectrophotometrically with either a Cary 14, Perkin-Elmer 320, or Hewlett-Packard 8450 spectrophotometer. Molar absorptivities of the copper(III)–Aib_3a complexes were determined by ascorbic acid titration and dilution. For longer wavelengths where it was not possible to prepare optically opaque solutions ($A > 3$), the quantum yield for loss of copper(III) was corrected for the fraction of light absorbed.[29] Corrections for inner-filter effects by the products[29] were made for solutions at pH 5 and 1.0 M OH^- and irradiation wavelengths ≤302 nm. For product determinations, the complexes were photolyzed to completion (i.e., no copper(III) left). After exhaustive photolysis samples of $Cu^{III}(H_{-2}Aib_3a)^+$ in 4.0 M $HClO_4$ and $Cu^{III}(H_{-4}Aib_3a)^-$ in 1.0 M OH^- were neutralized and diluted in the appropriate mobile-phase buffer. Ferrioxalate actinometry[32] was used to determine the light intensity.

Chromatographic Analysis. The major peptide products of the photodecomposition were analyzed by reverse-phase HPLC. An IBM 9533/LC or a Varian 5000 was used with UV detection at 210 nm. Separation of the products was achieved on a Brownlee RP-300 Aquapore, 10-μ column (25 cm). Mobile phases were 0.02 M sodium phosphate buffer at pH values of 4.3, 5.4, or 6.2. Calibration curves, prepared from authentic compounds, used peak area measurements from a Hewlett-Packard 3390A integrator for quantitation of Aib_3a, Aib_3, Aib_2a, Aib_2, and **5**. One product, **6**, was identified by matching its retention behavior in different mobile phases to that of a hydantoin fragment isolated from the photodecomposition of $Cu^{III}(H_{-2}Aib_3)$ at pH 9.[29] The amide form of this hydantoin, **7**, is assigned as another major product. Neither of these hydantoins are available commercially. The percent recoveries of the two substituted hydantoins were determined by estimating their respective detector response as follows: First, the total amount of **6** and **7** in the product analysis at pH 5 and at a given irradiation wavelength is assumed to equal the difference in total initial peptide and that recovered as Aib_3a, Aib_2a, and **5**. This assumption is valid since no other peaks were observed. This amount of peptide recovered as **6** and **7** was different at nearly every irradiation wavelength. In addition, the peak area fractions for **6** and **7** varied as a function of irradiation wavelength. Thus, the difference in total peptide recovered was equated to the sum of the peak area fractions (times the unknown detector response) at the five irradiation wavelengths. The detector responses (two unknown) were then determined by solving the simultaneous equations. The percent recoveries reported for **6** and **7** are based on these estimates for the detector responses and the total copper(III) lost.

Kinetic Measurements. The protonation kinetics of $Cu^{III}(H_{-3}Aib_3a)$ to $Cu^{III}(H_{-2}Aib_3a)^+$ were measured with a Perkin-Elmer 320 spectrophotometer interfaced to a Perkin-Elmer 3600 data station or a Durrum stopped-flow spectrophotometer interfaced to a Hewlett-Packard 2108 microcomputer. The reactions were studied at 25.0 ± 0.2 °C under pseudo-first-order conditions with acid ($HClO_4$) in excess. Ionic strength was maintained at 2.0 M with $NaClO_4$. The reported rate constants are an average of at least three trials at the same conditions.

The deprotonation kinetics of $Cu^{III}(H_{-3}Aib_3a)$ to $Cu^{III}(H_{-4}Aib_3a)^-$ were studied with a pulsed-accelerated-flow spectrometer.[33,34] This continuous-flow method with integrating observation has been used to measure first-order rate constants of up to 120 000 s^{-1}. The reaction was

(30) Hamburg, A. W.; Nemeth, M. T.; Margerum, D. W. *Inorg. Chem.* **1983**, *22*, 3535–3544.
(31) Bossu, F. P.; Margerum, D. W. *Inorg. Chem.* **1977**, *16*, 1210–1214.
(32) Calvert, J. G.; Pitts, J. N., Jr. *Photochemistry*; Wiley: New York, 1966; pp 783–785.
(33) Jacobs, S. A.; Nemeth, M. T.; Kramer, G. W.; Ridley, T. Y.; Margerum, D. W. *Anal. Chem.* **1984**, *56*, 1058–1065.
(34) Nemeth, M. T.; Fogelman, K. D.; Ridley, T. Y.; Margerum, D. W., submitted for publication in *Anal. Chem.*

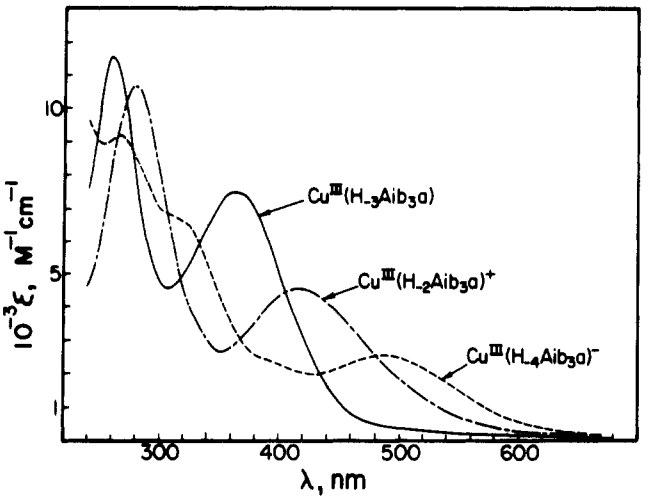

Figure 1. Ultraviolet–visible absorption spectra for the three forms of copper(III)–Aib_3a: $Cu^{III}(H_{-3}Aib_3a)$ in 0.050 M acetate buffer, pH 5.0, μ = 0.10 M ($NaClO_4$) (—); $Cu^{III}(H_{-2}Aib_3a)^+$ in 4.0 M $HClO_4$ (-·-); $Cu^{III}(H_{-4}Aib_3a)^-$ in 1.0 M OH^- (---).

studied at 25.0 ± 0.2 °C under pseudo-first-order conditions with base (NaOH) in excess. Ionic strength was maintained at 0.50 M with $NaClO_4$.

Results and Discussion

Three Forms of $Cu^{III}Aib_3a$. The ultraviolet–visible absorption spectrum for a solution of $Cu^{III}(H_{-3}Aib_3a)$ (**1**) in 0.050 M acetate buffer, pH 5.0, μ = 0.10 M ($NaClO_4$), exhibits intense absorption bands at 260 and 364 nm (Figure 1). The high oxidation state of the metal, the large molar absorptivities of the bands, and comparison with several other copper(III) peptide complexes, as well as other d^8 transition-metal halide complexes,[35] have indicated the transitions are of ligand-to-metal charge-transfer (LMCT) character. The chromophore structure is assigned to the Cu(III)–N(peptide) unit, which has both σ- and π-symmetry molecular orbitals relative to the metal–peptide nitrogen bond.[29] The high-energy band is designated as a σ-LMCT transition, and the low-energy band as a π-LMCT transition. (If a LMCT transition from the amine nitrogen exists, then its energy must overlap with that from the N(peptide).[29])

In high acid, $Cu^{III}(H_{-3}Aib_3a)$ undergoes a spectral change, which is consistent with protonation of the terminal amide nitrogen to give $Cu^{III}(H_{-2}Aib_3a)^+$ (**3**) (eq 1). Three isosbestic points are

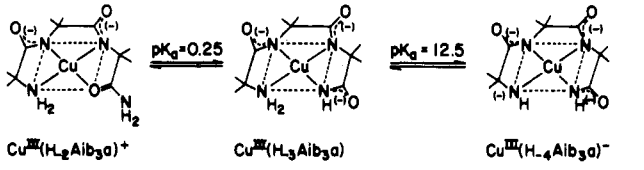

(1)

observed as the two LMCT bands are red shifted, relative to $Cu^{III}(H_{-3}Aib_3a)$, with increasing acid concentration.[36] This red shift is indicative of loss of coordination of a peptide nitrogen and replacement by a weaker donor, which is in accord with earlier reports on the spectral differences between tripeptides and tetrapeptides of copper(III)[29] and the effect of acid on nickel(III) peptides.[37] Not surprisingly then, the resultant transition maxima for $Cu^{III}(H_{-2}Aib_3a)^+$ at 278 and 415 nm (see Figure 1) are very similar to the bands observed for $Cu^{III}(H_{-2}Aib_3)$ (**2**) at 278 and 395 nm, as are the structures of the two complexes. (No shifts of the LMCT bands are observed for **2** in 4.0 M $HClO_4$, but the molar extinction coefficient of the π-LMCT band decreases by ~10%. If a LMCT transition from O(carbonyl) exists, then its energy must overlap with that from the N(peptide).[29]) A pK_a value of 0.25 was determined spectrophotometrically on the basis of the loss of one proton from $Cu^{III}(H_{-2}Aib_3a)^+$.

The thermal redox stability of $Cu^{III}(H_{-2}Aib_3a)^+$ is also remarkably high relative to that of other copper(III) peptides. In 4.0 M $HClO_4$, where 88% of the complex is in the protonated form, less than 5% loss of copper(III) is observed in a 24-h period. Furthermore, after about 2 weeks, apart from the absorbance loss, the visible LMCT band has slightly blue shifted and broadened to a maximum of 395–410 nm. This shift is believed to be a result of acid hydrolysis of the terminal amide group to give the copper(III) tripeptide complex and ammonia.

As the pH increases, $Cu^{III}(H_{-3}Aib_3a)$ undergoes a color change from gold to red. This change is consistent with deprotonation of the coordinated terminal amine nitrogen to give the stable complex $Cu^{III}(H_{-4}Aib_3a)^-$ (**4**) (eq 1). The absorption spectrum for $Cu^{III}(H_{-4}Aib_3a)^-$ is also given in Figure 1 and is very similar to vidicon spectra obtained in the base decomposition of several glycyl and alanyl copper(III) complexes.[19] The change in the absorption spectrum as a function of hydroxide concentration was examined; four isosbestic points were evident,[36] which indicated the presence of only two absorbing stable species (eq 1). On the basis of a spectrophotometric titration, the pK_a for deprotonation of the terminal amine nitrogen was found to be 12.5. This value is similar to the pK_a values observed for the amine deprotonation of other copper(III) peptides.[19]

Ligand-to-metal π bonding has been proposed for the deprotonated amine nitrogen in similar copper(III) peptides.[19] Deprotonation of the nitrogen allows rehybridization of the nitrogen orbitals, such that the free electron pair resides in the nitrogen $2p_z$ orbital. This permits π interaction with the empty copper(III) $4p_z$ orbital. The energy levels of these orbitals are brought closer together by the negative charge on the nitrogen and the high oxidation state of the metal. The transition from this π-NH(−) orbital to the lowest unfilled metal d orbital ($d_{x^2-y^2}$) is then of lower energy than for the LMCT transitions from the σ- and π-N(peptide) chromophore orbitals. Thus, the new band at 486 nm is assigned as the π-deprotonated amine nitrogen LMCT.

A major difference between $Cu^{III}(H_{-4}Aib_3a)^-$ and other copper(III) deprotonated amine peptide complexes is the relative stability with respect to redox decomposition. $Cu^{III}(H_{-4}Aib_3a)^-$ is remarkably stable in high base (1.0 M OH^-) and shows very little loss of copper(III) for periods of weeks when stored in the dark. By contrast, the $Cu^{III}(H_{-4}G_4)^{2-}$ complex has a half-life of only 31 s in 0.5 M NaOH.[18] The estimated dark redox decomposition rate constant for $Cu^{III}(H_{-4}Aib_3a)^-$ is $<2 \times 10^{-7}$ s^{-1} at pH 12.[38] As indicated above, the deprotonated amine complexes of most other copper(III) peptides are short-lived and were observed only by stopped-flow vidicon spectroscopy. The rapid self-redox reaction for these other peptide complexes is base-catalyzed and gives copper(II) and oxidized ligand as products. The principal site of decomposition occurs in the third residue from the amine terminus. A linear correlation is observed for the log of the rate constant of base decomposition and the copper(III/II) reduction potential for a wide variety of copper peptides.[39] Hence, the low potential for the Aib_3a complex is consistent with its thermal stability.

The enhanced thermal redox stability of the copper(III)–Aib_3a complexes, in comparison to that of other copper(III) peptides, is attributed to the replacement of the α-carbon hydrogens on the peptide by methyl groups. First, the inductive properties of the α-carbon methyl groups increase the basicity of the peptide, relative to glycyl and alanyl peptides.[30] This results in greater electron donation by the coordinated groups to the metal. A decrease of 0.04 Å in the equatorial bond lengths is observed when the copper(II) peptide is changed from tetraglycine to Aib_3.[16,40]

(35) Gray, H. B. *Transition Met. Chem. (N.Y.)* **1965**, *1*, 240–287.
(36) Margerum, D. W. *Pure Appl. Chem.* **1983**, *55*, 23–34.
(37) Subak, E. J., Jr.; Loyola, V. M.; Margerum, D. W. *Inorg. Chem.* **1985**, *24*, 4350–4356.
(38) Fogelman, K. D.; Margerum, D. W., unpublished results.
(39) Nagy, J. C.; Diaddario, L. L.; Margerum, D. W., manuscript in preparation.

Table I. Rate Data for the Protonation of $Cu^{III}(H_{-3}Aib_3a)$[a]

$[HClO_4]$, M	k_{obsd}, s^{-1}	$[HClO_4]$, M	k_{obsd}, s^{-1}
0.0474	0.0141 ± 0.0001	0.569	0.0270 ± 0.0001
0.0948	0.0154 ± 0.0001	0.759	0.0306 ± 0.0001
0.284	0.0207 ± 0.0001		

[a] μ = 2.0 M ($NaClO_4$); $[Cu^{III}Aib_3a]_{total}$ = 6.0 × 10^{-5} M; 25.0 °C.

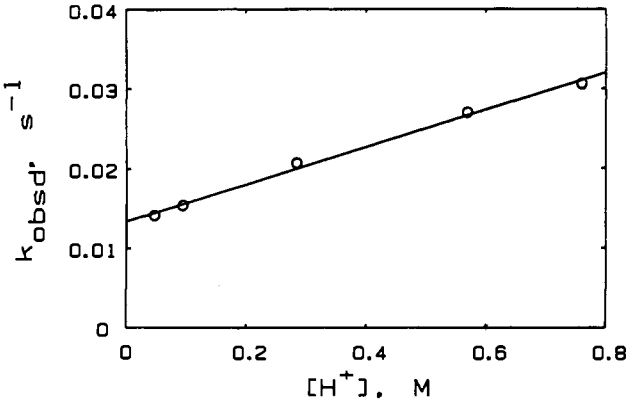

Figure 2. Hydrogen ion dependence of the observed rate constant for the protonation of $Cu^{III}(H_{-3}Aib_3a)$ to $Cu^{III}(H_{-2}Aib_3a)^+$ (eq 2–4).

Also, the higher oxidation state of copper has a greater affinity for this electron donation. An additional shortening of 0.09 Å in the average equatorial bond distances is observed for the Aib_3 complexes when the oxidation state of the copper is changed from +2 to +3.[4,16] Moreover, the ligand is less susceptible to oxidative fragmentation due to the absence of abstractable protons on the α-carbons. In contrast to this thermal stability, copper(III)–Aib_3a is very sensitive to photochemical decomposition by ultraviolet and visible radiation.

Kinetics of $Cu^{III}(H_{-3}Aib_3a)$ Protonation. The protonation of $Cu^{III}(H_{-3}Aib_3a)$ to $Cu^{III}(H_{-2}Aib_3a)^+$ (eq 2) was studied by monitoring the disappearance of $Cu^{III}(H_{-3}Aib_3a)$ at 364 nm in 0.050–0.80 M $HClO_4$. The reaction is first order in the cop-

$$Cu^{III}(H_{-3}Aib_3a) + H^+ \underset{k_{-1}}{\overset{k_1}{\rightleftharpoons}} Cu^{III}(H_{-2}Aib_3a)^+ \quad (2)$$

per(III) complex with a rate expression defined by eq 3. The

$$\frac{-d[Cu^{III}(H_{-3}Aib_3a)]}{dt} = k_{obsd}[Cu^{III}(H_{-3}Aib_3a)] \quad (3)$$

kinetic data under these conditions are summarized in Table I. A plot of the observed pseudo-first-order rate constants vs. the acid concentration (eq 4) is shown in Figure 2. Linear regression

$$k_{obsd} = k_1[H^+] + k_{-1} \quad (4)$$

of the data in Figure 2 yields k_1 = 0.023 (±0.001) M^{-1} s^{-1} and k_{-1} = 0.013 (±0.004) s^{-1}. The protonation equilibrium constant, K_H, is equal to k_1/k_{-1} = 1.77 M^{-1}. From these data a kinetic determination of the pK_a = 0.248 is found, which is in excellent agreement with the spectrophotometric value of 0.25.

The small value for the protonation rate constant reflects the inertness for equatorial substitution reactions of copper(III) peptides. In general, subsequent substitution or proton-transfer reactions are not observed prior to self-redox decomposition. The proton-transfer rate constant for the corresponding copper(II) complex, $Cu^{II}(H_{-3}Aib_3a)^-$, is nearly 10 orders of magnitude faster with k = 1.7 × 10^8 M^{-1} s^{-1}.[41] Furthermore, after the terminal amide nitrogen is protonated in the copper(II) peptide, stepwise dissociation of the peptide can be observed.

Rapid Rate of $Cu^{III}(H_{-3}Aib_3a)$ Deprotonation. The rate of the reaction of $Cu^{III}(H_{-3}Aib_3a)$ with OH^- to give the deprotonated

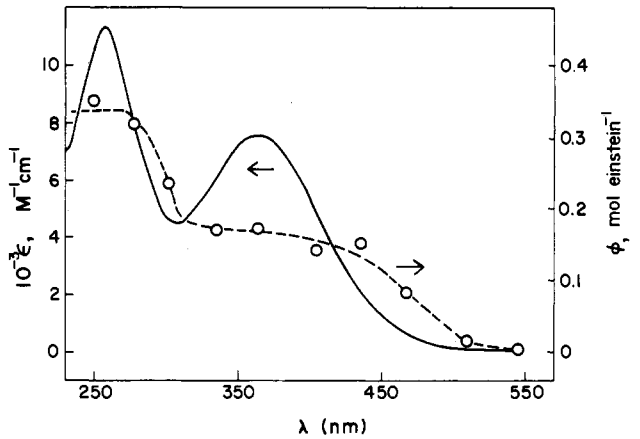

Figure 3. Disappearance quantum yield wavelength dependence (---) and UV–vis absorption spectrum (—) for $Cu^{III}(H_{-3}Aib_3a)$ in 0.050 M acetate buffer, pH 5.0, μ = 0.10 M ($NaClO_4$).

amine complex $Cu^{III}(H_{-4}Aib_3a)^-$ (eq 5) is too fast to measure by stopped-flow methods. This indicates that the k_2 value is greater

$$Cu^{III}(H_{-3}Aib_3a) + OH^- \underset{k_{-2}}{\overset{k_2}{\rightleftharpoons}} Cu^{III}(H_{-4}Aib_3a)^- \quad (5)$$

than 5 × 10^3 M^{-1} s^{-1}. The pulsed-accelerated-flow technique[33,34] was used with 0.010 M NaOH as a reactant under conditions where $(A_0 - A_\infty)$ values of 0.15 occurred at 500 nm. Again the deprotonation rate is too fast to measure, but these tests show that k_2 is greater than 10^5 M^{-1} s^{-1}.

Proton-transfer reactions from nitrogen bases are typically very fast. The second-order rate constant for the reaction of $^-OOCCH_2NH_3^+$ (pK_a = 9.8) with OH^- is 1.4 × 10^{10} M^{-1} s^{-1}.[42] In the present case we wished to see if the larger pK_a of 12.5 and the change of bonding between the copper(III) and the amine group after deprotonation in $Cu^{III}(H_{-4}Aib_3a)^-$ would cause a much slower proton-transfer reaction. The need to use relatively high hydroxide concentrations and the reversibility of the reaction limit the range of second-order rate constants that can be measured. Our results show that the k_2 value for $Cu^{III}(H_{-3}Aib_3a)$ is greater than 10^5 M^{-1} s^{-1}, but even with fast mixing techniques we cannot tell where the value falls between 10^5 and 10^{10} M^{-1} s^{-1}.

$Cu^{III}(H_{-3}Aib_3a)$ Photodecomposition. The quantum yield for loss of copper(III), Φ, has a marked wavelength dependence, as illustrated in Figure 3. This steplike behavior, where Φ for irradiation into the σ-LMCT band (0.36) is greater than Φ for the π-LMCT band (0.17) and then drops off at even longer wavelengths, is similar to the wavelength dependence reported for copper(III) tripeptide complexes.[29] The biplateau behavior is explained by the population of different excited states, each with its own distinct reactivity toward decomposition. The identity of the excited states or primary photoproducts is determined by the type of transition irradiated. Thus, on the basis of the ligand-to-metal charge-transfer character of the two transitions, the proposed metal–N(peptide) chromophore structure, and the respective symmetry designation for each transition, the primary photoproducts are described as σ- or π-copper(II) amidyl radicals, σ-$Cu^{II}L^{\bullet *}$ or π-$Cu^{II}L^{\bullet *}$ (structures **8**–**13** in Figure 4). This description of the excited states is consistent with the higher reactivity within the σ-LMCT band because there is already significant bond breaking (dissociation of L from the metal) in σ-$Cu^{II}L^{\bullet *}$, whereas in π-$Cu^{II}L^{\bullet *}$ the lone electron is delocalized over the π-bonding network.

The copper(II)–amidyl radicals can return to the copper(III) ground state radiatively and/or nonradiatively, as well as undergo ligand fragmentation and/or dissociation. Emission, both at room temperature and in a frozen glass, has not been observed for this and other d^8 copper(III) peptides upon excitation into either LMCT band under O_2-free conditions. Therefore, only decom-

(40) Freeman, H. C.; Taylor, M. R. *Acta Crystallogr.* **1965**, *18*, 939–952.
(41) Kumar, K.; Margerum, D. W., manuscript in preparation.
(42) Eigen, M. *Angew. Chem., Int. Ed. Engl.* **1964**, *3*, 1–19.

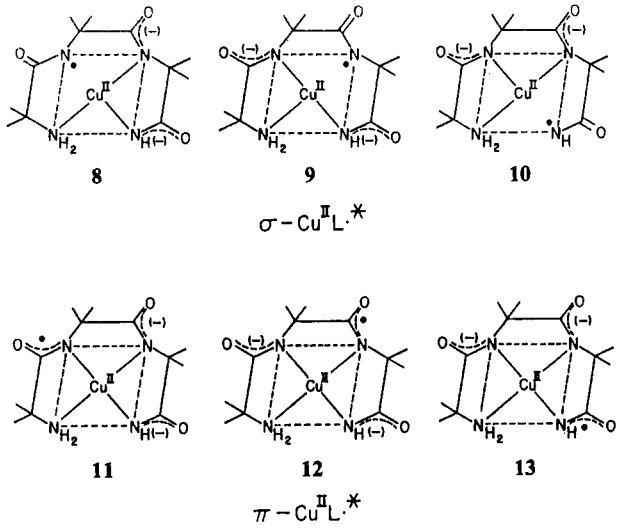

Figure 4. Structures for the σ- and π-copper(II) amidyl radical excited states.

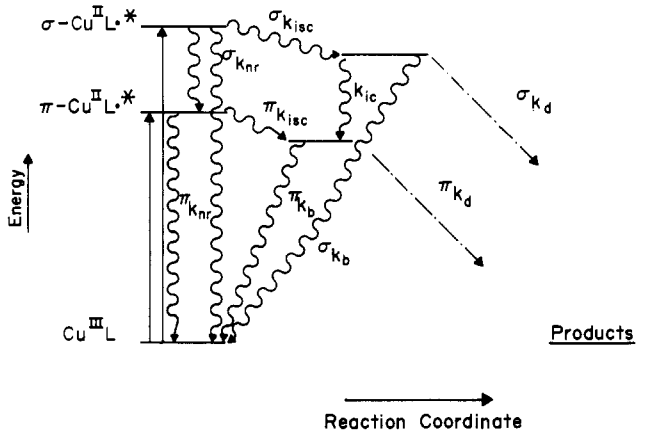

Figure 5. Simplified Jablonski diagram showing competition between nonradiative transitions (~) and reaction pathways (-·-) in the photodecomposition mechanism of copper(III) peptides with σ- and π-LMCT excited states. Solid lines (—) represent the absorption of light.

position competes with nonradiative decay of the excited state. A simple Jablonski diagram that describes the photochemical processes for $Cu^{III}(H_{-3}Aib_3a)$ is presented in Figure 5. The rate constants k_{nr}, k_{isc}, k_{ic}, k_b, and k_d designate respectively nonradiative relaxation from the Franck–Condon states or primary photoproducts, intersystem crossing to the longer-lived vibrationally equilibrated excited states, interconversion between the σ and π states, back-nonradiative relaxation to the ground state from the vibrationally equilibrated states, and decomposition, which includes dissociation and fragmentation paths. On the basis of symmetry restrictions[43] and previous work,[29] interconversion between the σ- and π-vibrationally equilibrated states, σ-$Cu^{II}L^{\bullet}$ and π-$Cu^{II}L^{\bullet}$, is believed to be small. If k_{ic} is neglected, then the quantum yield for loss of copper(III) is defined by eq 6, where $\Phi_{isc} = k_{isc}/(k_{nr}$

$$\Phi = \Phi_{isc}[k_d/(k_d + k_b)] \quad (6)$$

$+ k_{isc})$. If ${}^{\sigma}\Phi_{isc} \approx {}^{\pi}\Phi_{isc}$, then the higher quantum yield for σ-LMCT irradiation vs. π-LMCT irradiation indicates that ${}^{\sigma}k_d > {}^{\pi}k_d$ and/or ${}^{\sigma}k_b < {}^{\pi}k_b$. This difference in rate constants is plausible since formation of σ-$Cu^{II}L^{\bullet}$ requires some degree of bond breaking, whereas stabilization of π-$Cu^{II}L^{\bullet}$ occurs through the π-bonding.

For $Cu^{III}(H_{-3}Aib_3a)$, the major products from the photoinduced decomposition arises from fragmentation at the same three sites as those reported for the copper(III) tripeptides[29] (see Figure 6). The percent recovery for each of the major products, based on the amount of copper(III) lost, is summarized in Table II with

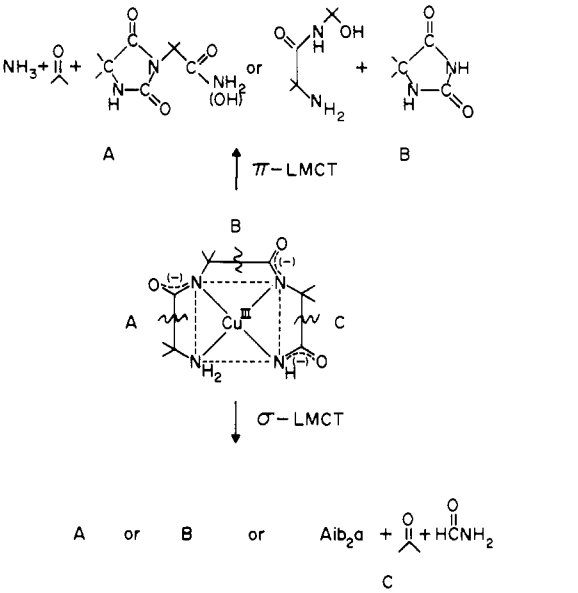

Figure 6. Fragmentation sites for σ- and π-LMCT irradiation of $Cu^{III}(H_{-3}Aib_3a)$ at pH 5.

Table II. Wavelength Dependence on the Photodecomposition Stoichiometry of $Cu^{III}(H_{-3}Aib_3a)$ at pH 5[a]

	% recovery[b]					
λ, nm	Aib_2a	**5**	**6**	**7**	Aib_3a	total
278	9	23	7	14	50	103
302	8	20	6	15	51	100
366	7	17	5	21	50	100
405	4	16	5	23	51	99
436	2	16	6	24	51	99
error	±1	±2	±3	±3	±1	

[a] Complete photolysis of $Cu^{III}(H_{-3}Aib_3a)$ in 0.10 M acetate buffer at pH 5.0. [b] Based on the amount of Cu(III) lost.

reference to the wavelength of irradiation. Although the sites of cleavage are the same as for the tripeptides, the products are different. Hydantoins (**5**–**7**) account for almost half (40–48%) of the total peptide. The other half is recovered as the parent peptide, Aib_3a, independent of wavelength. This recovery of 50% of Aib_3a indicates that a ground-state $Cu^{III}L$ complex is reduced rapidly by $Cu^{II}L^{\bullet}$ (or with fragments from $L^{\bullet}$) to give two copper(II) ions, an intact parent peptide L, and oxidized fragments of L (i.e., hydantoins).

Previously, hydantoins were not observed in the photodecomposition of copper(III) tripeptides at pH 5 and 1.[29] However, under alkaline conditions (pH 9), hydantoin **6** was found as the major product in the photolysis of $Cu^{III}(H_{-2}Aib_3)$.[29] Only at pH values where the peptide would remain coordinated to the copper(II) (i.e., pH greater than the last ligand pK_a) was formation of the hydantoin thought possible. $Cu^{II}Aib_3a$ has a log K_1 value of 4.42 and pK_{a1}, pK_{a2}, and pK_{a3} values of 4.71, 7.34, and 7.97, respectively.[30] At pH 5 considerable dissociation of the ligand fragments from copper(II) would be expected on the basis of these pK_a values. Nonetheless, hydantoins are observed as the major product in the photodecomposition of $Cu^{III}(H_{-3}Aib_3a)$ at pH 5.

Hydantoin **5** is 5,5-dimethylhydantoin. It is believed to form from cleavage at site B (Figure 6). Fragmentation at this position would lead to an isocyanate intermediate, **14**, which we propose undergoes a nucleophilic cyclization with the terminal deprotonated amide nitrogen (eq 7). A space-filling model shows that

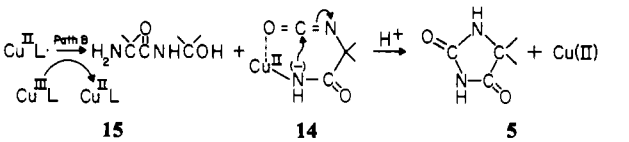

(7)

(43) Skell, P. S.; Day, J. C. *Acc. Chem. Res.* **1978**, *11*, 381–387.

to get close approach of the deprotonated peptide nitrogen to the isocyanate carbon, the isocyanate oxygen comes near enough to indicate an O–Cu(II) interaction. Such an interaction should facilitate the reaction because electron density from the oxygen shifts toward the copper. This would make the isocyanate carbon more electropositive and hence more susceptible to nucleophilic attack. Further evidence to support a metal-assisted path in hydantoin formation is the observation of hydantoin **6** in the photodecomposition of $Ni^{III}(H_{-2}Aib_3)$ at pH 1.[44] Dissociation of the ligand fragments from nickel(II) is expected to be slow since the dissociation reactions of nickel(II) peptide complexes in acid solution are very sluggish.[45]

Hydantoins are generally prepared from a bimolecular reaction of an isocyanate, R'NCO, and an amino acid (eq 8) under mildly alkaline conditions in an organic/aqueous solvent mixture;[46] the amino nitrogen is the nucleophile. Under acidic conditions the

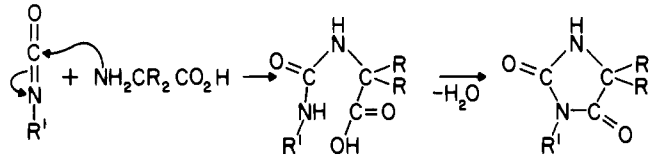

(8)

amino acid exists as the zwitterion, and the protonated amine group no longer acts as a nucleophile. In addition, the isocyanate group is susceptible to acid-catalyzed hydrolysis. There are no previous examples of an intramolecular nucleophilic reaction by an amide nitrogen on an isocyanate group to form a hydantoin. Although amide nitrogens are much poorer nucleophiles than amine nitrogens, deprotonation of a nitrogen and coordination to a metal can enhance its nucleophilicity. Nucleophilic reactions by the deprotonated amine nitrogen coordinated to copper(III) in $Cu^{III}(H_{-4}G_4)^{2-}$ have been observed.[47] We believe this mechanism for hydantoin formation is the first example of a nucleophilic reaction by a metal-coordinated deprotonated peptide nitrogen. There is, however, a precedent for cyclization reactions where a coordinated amide acts as a nucleophile in studies of the base hydrolysis of the 1,2-dicyanobenzene complex of cobalt(III) pentaammine.[48,49] The reaction in eq 9 was reported after the

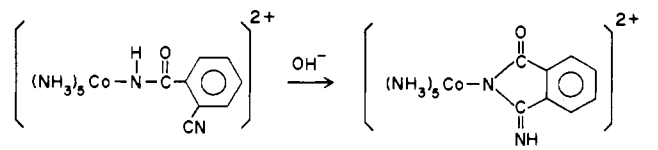

(9)

initial hydrolysis occurred. The cyclic ligand formed is 1-oxo-3-iminoisoindoline rather than the hydantoin formed from the peptide decomposition reactions, but the reaction illustrates the reactivity of the coordinated amide nitrogen.

In addition to 5,5-dimethylhydantoin (**5**), formation of a *N*-(hydroxyalkyl)amide, $H_2NC(CH_3)_2CONHC(CH_3)_2OH$ (**15**), intermediate will result from cleavage at B. This intermediate will rapidly hydrolyze to Aiba and acetone (eq 10). A similar species, $RCONHCH_2OH$, was found in the autoxidation of nickel(II) tetraglycine;[50] it was less susceptible to hydrolysis because the α-carbon was not substituted.

$$\underset{\mathbf{15}}{NH_2C(CH_3)_2CONHC(CH_3)_2OH} \xrightarrow{H^+, H_2O} \text{Aiba} + (CH_3)_2C{=}O \quad (10)$$

Formation of the 3-substituted hydantoin, **7**, is believed to result from cleavage at site A. Fragmentation at this position leads to the isocyanate intermediate, **16**, which undergoes intramolecular cyclization via nucleophilic attack by the deprotonated peptide nitrogen (eq 11). Again a space-filling model suggests an oxy-

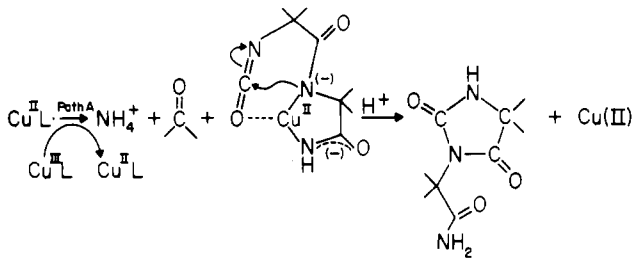

16 **7**

(11)

gen–copper interaction that would assist cyclization. This mechanism for formation of **7** is identical with the mechanism proposed for formation of **6** in the alkaline photolysis of $Cu^{III}(H_{-2}Aib_3)$.[29] The difference is that the mechanism proceeds at pH 5 for $Cu^{III}(H_{-3}Aib_3a)$ but not for $Cu^{III}(H_{-2}Aib_3)$. This indicates that coordination by the terminal deprotonated amide nitrogen, a significantly stronger donor than a carboxylate oxygen, facilitates this intramolecular reaction. Cyclization is more competitive than dissociation for the Cu(II) intermediate derived from Aib_3a, whereas the opposite must be true for the intermediate from Aib_3. Two possible explanations to account for the different products and/or mechanisms formed at pH 5 between these copper(III) peptide complexes are (1) coordination by the terminal deprotonated amide nitrogen increases the nucleophilic reactivity of the deprotonated peptide nitrogen in the Aib_3a species relative to coordination by the carboxylate oxygen in the Aib_3 species and (2) the lifetime of the coordinated isocyanate intermediate, **16**, is greater than the lifetime for the corresponding intermediate with the terminal carboxylate group (i.e. the fragment from $Cu^{III}(H_{-2}Aib_3)$ with cleavage at site A).

The formation of hydantoin **6** is explained as resulting from the hydrolysis of the terminal amide function in **7**. There is a degree of uncertainty in the recoveries of **6** and **7**. This is due to the fact that the amounts recovered were approximated by first estimating the detector response factor as described above. It is clear there is considerably less of **6** than of **7**. Hydrolysis of the parent peptide, Aib_3a, to Aib_3 is not observed under mild conditions (0.10 M acetate buffer, pH 5), so it is difficult to imagine that extensive hydrolysis of **7** would also occur.

The smaller peptide, Aib_2a, is also a product in the photodecomposition of $Cu^{III}(H_{-3}Aib_3a)$ at pH 5. It is the major product that results from fragmentation at site C. Although Aib_2a could also arise from cleavage at site A (in a pathway analogous to the generation of Aib_2, CO_2, $(CH_3)_2CO$, and NH_3 in the photodecomposition of **2**),[29] the intramolecular nucleophilic cyclization (eq 11) appears to be the predominant path instead.

The percent recovery of Aib_2a shows a wavelength dependence that parallels the wavelength dependence of **5**. Both of these products decrease with increasing wavelength of irradiation. This decrease in the effectiveness of fragmentation at sites B and C at lower energies is offset by an increase in the fragmentation at site A, as evidenced by an increase in the yields of **6** and **7**. Cleavage at site A was also found to be preferred within the lower energy π-LMCT band in the photodecomposition of copper(III) tripeptides.[29] The higher ratio of the 3-substituted hydantoins (**6**, **7**) to Aib_2a and **5** for irradiation in the π-LMCT band is attributed to preferential population of **11** vs. that of **12** and **13**. For irradiation in the σ-LMCT transition, similar product yields from site A (**6**, **7**) and site B (**5**) are obtained, but a considerably smaller yield from path C is observed. This distribution is attributed to preferential and similar population of **8** and **9** vs. that of **10**.

$Cu^{III}(H_{-2}Aib_3a)^+$ Photodecomposition. The photochemistry of $Cu^{III}(H_{-2}Aib_3a)^+$ was examined in 4.0 M $HClO_4$. Consequently,

(44) Hamburg, A. W. Ph.D. Thesis, Purdue University, 1982.
(45) Kennedy, W. R.; Margerum, D. W. *Inorg. Chem.* **1985**, *24*, 2490–2495.
(46) Ware, E. *Chem. Rev.* **1950**, *46*, 403–470.
(47) Kirksey, S. T., Jr.; Margerum, D. W. *Inorg. Chem.* **1979**, *18*, 966–970.
(48) Balahura, R. J.; Purcell, W. L. *Inorg. Chem.* **1979**, *18*, 937–941.
(49) Balahura, R. J.; Purcell, W. L. *Inorg. Chem.* **1981**, *20*, 4159–4163.
(50) Bossu, F. P.; Paniago, E. B.; Margerum, D. W.; Kirksey, S. T., Jr.; Kurtz, J. L. *Inorg. Chem.* **1978**, *17*, 1034–1042.

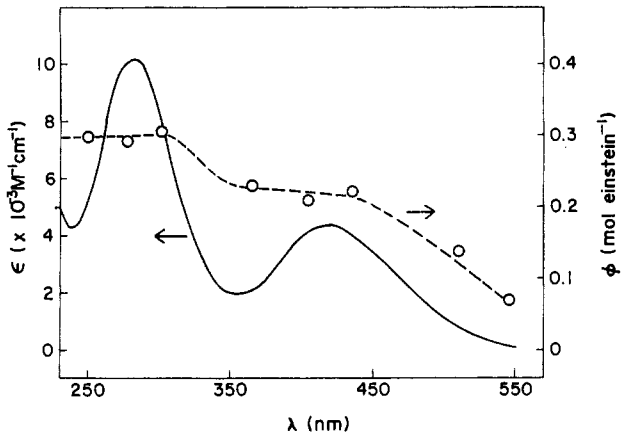

Figure 7. Corrected disappearance quantum yield wavelength dependence (---) and UV–vis absorption spectrum (—) for $Cu^{III}(H_{-2}Aib_3a)^+$ in 4.0 M $HClO_4$.

with a pK_a of 0.25, only 88% of the total copper(III) present is in the protonated or H_{-2} form. The quantum yield for total loss of copper(III), Φ(Cu), was measured as a function of wavelength and is assumed to be a simple composite of the quantum yields for both $Cu^{III}(H_{-3}Aib_3a)$ (Φ(H_{-3})) and $Cu^{III}(H_{-2}Aib_3a)^+$ (Φ(H_{-2})) on the basis of their distribution in solution as defined in eq 12.

$$\Phi(Cu) = 0.88\Phi(H_{-2}) + 0.12\Phi(H_{-3}) \quad (12)$$

With Φ(H_{-3}) from above (Figure 3), the quantum yield for loss of $Cu^{III}(H_{-2}Aib_3a)^+$ was determined and is plotted with reference to its absorption spectrum in Figure 7. (These corrected quantum yields for the H_{-2} form vary less than 5% from the measured quantum yield for total loss of copper(III).) Again the biplateau effect is observed, where $\Phi(\sigma) > \Phi(\pi)$. However, the difference in reactivity between the two excited states is considerably less than for $Cu^{III}(H_{-3}Aib_3a)$ (i.e., $\Phi(\sigma) - \Phi(\pi) = 0.08$ for $Cu^{III}(H_{-2}Aib_3a)^+$ as compared to 0.19 for $Cu^{III}(H_{-3}Aib_3a)$). Furthermore, Φ(σ) for the H_{-2} form is only about 80% of Φ(σ) for the H_{-3} form, whereas Φ(π) is 30% greater.

Previously, it was found that ligand structural variations affect the quantum yield for loss of copper(III).[29] As the number of hydrogens bonded to the α-carbons on the peptide backbone increased, a general decrease was seen for Φ(σ) and Φ(π). This effect was more pronounced for Φ(π) than for Φ(σ) and was attributed to enhancement of the nonradiative relaxation of the excited states by α-C–H vibrations. In this case there is no change in the number of α-carbon hydrogens; instead, there is a change in the coordination about the metal. The terminal deprotonated amide nitrogen in $Cu^{III}(H_{-3}Aib_3a)$ is protonated and replaced by the carbonyl oxygen in $Cu^{III}(H_{-2}Aib_3a)^+$.

The UV–vis absorption spectrum of $Cu^{III}(H_{-2}Aib_3a)^+$, not surprisingly, resembles the spectrum for $Cu^{III}(H_{-2}Aib_3)$;[29] both have an oxygen coordinated to the metal, as described above. In addition to these similarities, the magnitudes of their respective quantum yields are also found to be very similar. (For $Cu^{III}(H_{-2}Aib_3)$, $\Phi(\sigma) = 0.34$ and $\Phi(\pi) = 0.23$ mol einstein^{-1}.)[29] Hence, it is apparent from the comparison of Φ for $Cu^{III}(H_{-3}Aib_3a)$, $Cu^{III}(H_{-2}Aib_3a)^+$, and $Cu^{III}(H_{-2}Aib_3)$, all of which have the same number of α-carbon methyl groups on the peptide backbone, that the quantum yield also depends on the type of donor group coordinated to the metal at the fourth position. (Positions are numbered beginning with the amine nitrogen.)

The difference in the quantum yields for these complexes can be attributed to differences in the rate constants for the various competing processes. The photochemical decomposition mechanism depicted in Figure 5 is general and is applicable to $Cu^{III}(H_{-2}Aib_3a)^+$ as well as other copper(III) peptides with similar σ- or π-LMCT states. Hence, coordination by a deprotonated amide nitrogen in the fourth position can be viewed as stabilizing π-$Cu^{II}L^{\cdot+}$ and/or enhancing its rate of nonradiative relaxation to the ground state relative to coordination by a carbonyl or carboxylate oxygen in that position. In terms of the rate processes, ${}^{\pi}k_{nr} > {}^{\sigma}k_{nr}$ such that the assumption ${}^{\pi}\Phi_{isc} \approx {}^{\sigma}\Phi_{isc}$ is not valid and/or ${}^{\pi}k_b$ for $Cu^{III}(H_{-3}Aib_3a)$ is increased relative to ${}^{\pi}k_b$ for $Cu^{III}(H_{-2}Aib_3a)^+$. In contrast, the same coordination by the deprotonated nitrogen appears to enhance the reactivity of σ-$Cu^{II}L^{\cdot+}$ (i.e., ${}^{\sigma}k_d$ for $Cu^{III}(H_{-3}Aib_3a)$ is increased relative to ${}^{\sigma}k_d$ for $Cu^{III}(H_{-2}Aib_3a)^+$).

Table III. Wavelength Dependence on the Photodecomposition Stoichiometry of $Cu^{III}(H_{-2}Aib_3a)^+$ in 4.0 M $HClO_4$[a]

	% recovery[b]				
λ, nm	Aib_2	Aib_2a	Aib_3	Aib_3a	total[c]
278	2	25	5	45	77
302	<1	20	4	48	72
366	<1	25	5	46	76
436	<1	22	3	46	71
error	±1	±2	±1	±1	

[a] Complete photolysis of $Cu^{III}(H_{-2}Aib_3a)^+$ in 4.0 M $HClO_4$. [b] Based on the amount of Cu(III) lost. [c] Aib and Aiba are proposed to account for the remaining peptide (see text for discussion).

The major peptide products from the photoinduced decomposition of $Cu^{III}(H_{-2}Aib_3a)^+$ in 4.0 M $HClO_4$ as a function of photolysis wavelength are summarized in Table III. Almost half of the total peptide is recovered intact. No hydantoins are detected, and there is no apparent wavelength dependence on formation of any of the products.

The conditions for this photodecomposition are severe, so it is not surprising that some of the parent peptide is hydrolyzed to Aib_3. The sum of the recoveries of Aib_3 and Aib_3a equals 50%. The absence of hydantoin products can be explained by two circumstances. First, under these conditions rapid dissociation of L$^{\cdot}$ or the isocyanate fragment from copper(II) is expected. Thus, dissociation is more competitive than intramolecular nucleophilic cyclization. In addition, the fully protonated, uncoordinated terminal amide nitrogen is an ineffective nucleophile and thus unable to induce intramolecular cyclization after cleavage at site B.

A major product observed in the photolysis of $Cu^{III}(H_{-2}Aib_3a)^+$ is Aib_2a. The lack of a wavelength dependence on the recovery of Aib_2a can be explained by the fact that there are two competing paths that form Aib_2a. With the absence of hydantoin formation, Aib_2a is the predicted product from cleavage at site A; it forms from hydrolysis of the uncoordinated isocyanate intermediate, **17** (eq 13). As in the photolysis of $Cu^{III}(H_{-3}Aib_3a)$, Aib_2a also forms

$$\underset{\mathbf{17}}{O{=}C{=}NC(CH_3)_2CONHC(CH_3)_2CONH_2} \xrightarrow{H^+,\,H_2O} CO_2 + Aib_2a \quad (13)$$

from cleavage at C. These paths showed opposite wavelength preference in Table II. Thus, while the amount of Aib_2a from cleavage at site C decreases with increasing wavelength of irradiation, more Aib_2a is formed from the preferred cleavage site, A. The net effect is an essentially constant yield of Aib_2a regardless of the photolysis wavelength.

Almost a quarter of the total peptide is unaccounted for by the HPLC separation. The missing peptide is believed to be primarily Aiba and Aib. Two equivalents of Aiba are expected from cleavage at B; 1 equiv by hydrolysis of the uncoordinated isocyanate intermediate, **18** (eq 14), instead of cyclization to form

$$\underset{\mathbf{18}}{O{=}C{=}NC(CH_3)_2CONH_2} \xrightarrow{H^+,\,H_2O} CO_2 + Aiba \quad (14)$$

5 and the other from hydrolysis of **15** (eq 10). Aib would arise from the hydrolysis of Aiba. Each of these species has only one chromophore (i.e., C=O); consequently, they each have a very weak detector response at 210 nm. Under ideal conditions for separation of the other peptides, Aiba and Aib in the sample are not observed because a large solvent background peak masks their much weaker signals. This solvent response is attributed to the large difference in ionic strength (and thus refractive index) between the sample (≈2 M, due to neutralization) and that of the mobile phase (0.02 M phosphate).

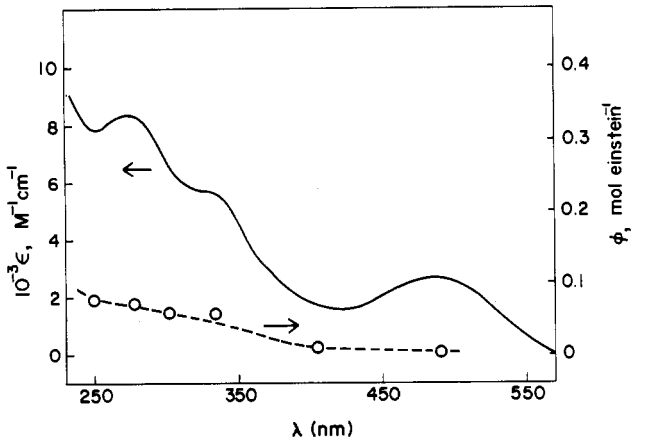

Figure 8. Disappearance quantum yield wavelength dependence (---) and UV-vis absorption spectrum (—) for $Cu^{III}(H_{-4}Aib_3a)^-$ in 1.0 M OH^-.

$Cu^{III}(H_{-4}Aib_3a)^-$ Photodecomposition. The quantum yield for loss of $Cu^{III}(H_{-4}Aib_3a)^-$ (**4**) in 1.0 M OH^- is illustrated in Figure 8 with reference to the absorption spectrum. The behavior of Φ is markedly different from that for the other two forms of Cu(III)–Aib_3a and the copper(III) tripeptides.[29] There is no biplateau behavior. Instead, a dramatic reduction in Φ is observed over all wavelengths. The quantum yield decreases with increasing wavelength and approaches zero at 490 nm (Φ < 0.004 mol einstein^{-1}). A similar reduction in Φ and lack of wavelength dependence has also been observed for another deprotonated amine copper(III) complex, that of Aib_3G, $Cu^{III}(H_{-4}Aib_3G)^{2-}$ (**19**).[51] Hence, this behavior is associated with copper(III) deprotonated amine complexes.

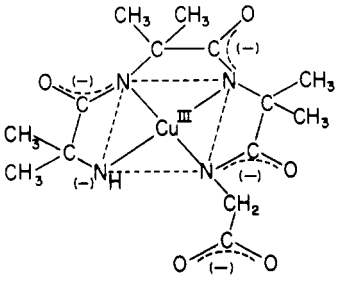

19

The reduction in Φ indicates that photochemical loss of copper(III) is much less efficient for the deprotonated amine complexes. This reduction in Φ could result from (1) the presence of some quencher or (2) the occurrence of additional, more competitive self-relaxation paths from the excited state. Oxygen, a possible trace contaminant in these argon-saturated solutions, does not behave as a quencher. The disappearance quantum yield is unaffected by saturation of oxygen for any of the forms of copper(III)–Aib_3a. However, oxygen is an efficient quencher of the photodecomposition of other copper(III) peptides[51] and $Ni^{III}(H_{-2}Aib_3)$.[44] The likelihood of a contaminant quencher in solution is small since $Cu^{III}(H_{-4}Aib_3a)^-$ is prepared simply by mixing $Cu^{III}(H_{-3}Aib_3a)$ in concentrated base. Hydroxide is necessary in such high concentrations in order to fully deprotonate the terminal amine nitrogen. Other anions (e.g., ClO_4^-, Cl^-, N_3^-) have no effect on Φ for $Cu^{III}(H_{-3}Aib_3a)$. The same low quantum yields are also observed if $Cu^{III}(H_{-4}Aib_3a)^-$ is prepared in 1.0 M OD^-/D_2O (≈98% D). Therefore, the reduction in Φ must result from other competitive self-relaxation processes.

One possible path is radiative relaxation. On the basis of Kasha's rule, emission could arise from the lowest excited state, which is the π-deprotonated amine, π-NH(−)–LMCT, transition. However, no emission is observed from $Cu^{III}(H_{-4}Aib_3a)^-$ in 1.0 M OH^- or 1.0 M OD^-/D_2O at room temperature or frozen with

(51) Hinton, J. P. Ph.D. Thesis, Purdue University, 1986.

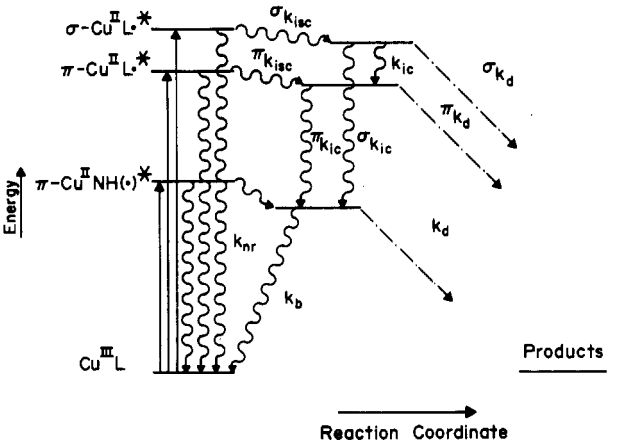

Figure 9. Simplified Jablonski diagram for the photodecomposition mechanism of copper(III) deprotonated amine peptide complexes. The back-nonradiative relaxation pathways to the ground state, $^{\sigma}k_b$ and $^{\pi}k_b$, have been omitted for clarity.

Table IV. Wavelength Dependence on the Photodecomposition Stoichiometry of $Cu^{III}(H_{-4}Aib_3a)^-$ in 1.0 M OH^- [a]

	% recovery[b]					
λ, nm	Aib_2 + Aib_2a	**5**	**6**	**7**	UNK[c]	Aib_3a
278	6	26	5	<2	13	48
334	9	20	8	<2	13	50
366	7	17	10	<2	16	49
436	11	10	11	<2	18	53
error	±2	±2	±3			±2

[a] Complete photolysis of $Cu^{III}(H_{-4}Aib_3a)^-$ in 1.0 M OH^-. [b] Based on the amount of Cu(III) lost. [c] UNK = 50 − (Aib_2 + Aib_2a + **5** + **6**).

excitation at 485 nm (π-NH(−)–LMCT) or 300 nm. A simple energy diagram for the possible photochemical processes of $Cu^{III}(H_{-4}Aib_3a)^-$ in 1.0 M OH^- is described by Figure 9, where the abbreviations for the rate constants are the same as defined previously. The absence of emission, lack of a quencher, and minimal photochemical loss of copper(III) at 490 nm indicate the deprotonated π-aminyl excited state is coupled efficiently to the ground state. This could be due to (1) a very small formation efficiency of the vibrationally equilibrated deprotonated amine excited state by intersystem crossing from the Franck–Condon state (i.e., $\Phi_{isc} \ll 1$ if k_{nr} is much greater than k_{isc}) and/or (2) the rate of back-nonradiative relaxation from the vibrationally equilibrated π-NH(•) state, k_b, being much greater than the product forming path(s) from this excited state, k_d. In order to explain the low copper(III) disappearance quantum yields over all wavelengths, the rates of interconversion, k_{ic}, from σ-$Cu^{II}L^•$ to π-$Cu^{II}L^•$ and from these states to the lower energy deprotonated π-aminyl excited state must be greater than their respective rates of decomposition. The previous symmetry restrictions for interconversion between the σ- and π-$Cu^{II}L^•$ excited states are now somewhat relaxed since the transitions for population of the Franck–Condon states (σ-$Cu^{II}L^{•*}$ and π-$Cu^{II}L^{•*}$) are poorly defined (i.e., they overlap in the UV–vis absorption spectrum); only the π-NH(−)–LMCT band is well-defined. Relaxation from LMCT states to the ground state by deactivation through lower excited states is not uncommon and has been reported for amine complexes of Co(III) and Rh(III).[52]

The products with their respective percent recoveries from the photodecomposition of $Cu^{III}(H_{-4}Aib_3a)^-$ in 1.0 M OH^- are summarized in Table IV. Again 50% of the parent peptide, Aib_3a, is recovered unchanged. This indicates that the step in which copper(III) is lost is essentially the same as for the other copper(III) peptides, but it just does not occur as often.

(52) Adamson, A. W.; Fleischauer, P. D., Eds. *Concepts of Inorganic Photochemistry*; Wiley: New York, 1975; pp 81–201 and references therein. Ford, P. C. *J. Chem. Educ.* **1983**, *60*, 829–833.

The remaining 50% of the ligand is distributed among five products. 5,5-Dimethylhydantoin is the major product, and it exhibits a similar wavelength profile as it did in the photolysis of $Cu^{III}(H_{-3}Aib_3a)$ (i.e., forming preferentially from σ-LMCT irradiation). The combination of Aib_2a and its hydrolysis product, Aib_2, accounts for a similar fraction of the total peptide and similar wavelength distribution that Aib_2a did in the photolysis at pH 5. Increasing amounts of **6** with increasing wavelength of irradiation are found, but **7** is not observed at any wavelength. Hydrolysis of **7** is the only mechanism for formation of **6**. Thus, **7** may be present but at the limit of detection. An unknown product, UNK, is observed, and the amount of UNK increases with increasing wavelength. In mobile phase at pH 5.4, UNK has a retention time between those of Aib_3a and Aib_3; at pH 6.2, its retention time decreases slightly and falls between those of Aib_2a and Aib_3. On the basis of its wavelength dependence and the smaller recovery of the 3-substituted hydantoins from cleavage at site A (relative to the H_{-3} form), UNK is believed to form from decomposition of the deprotonated π-aminyl excited state.

Conclusions

The photoredox decomposition of copper(III) peptides is shown to be strongly dependent on the type of donor groups coordinated to the metal. Not only can the trivalent oxidation state of copper be stabilized in aqueous solution toward redox decomposition (in the dark) by coordination to Aib_3a, but in addition the copper(III) peptide can be stabilized toward light-induced redox decomposition by deprotonation of the terminal amine nitrogen. The deprotonated amine complex, $Cu^{III}(H_{-4}Aib_3a)^-$, is significantly less sensitive to UV-vis irradiation than are the other two forms of copper(III)-Aib_3a. The decrease in photoreactivity is attributed to rapid interconversion of the σ- and π-copper(II) amidyl states to the lower energy π-deprotonated aminyl state, which is coupled efficiently to the ground state.

Hydantoins are the principal peptide oxidation products from photolysis of $Cu^{III}(H_{-3}Aib_3a)$ at pH 5 and $Cu^{III}(H_{-4}Aib_3a)^-$ in 1.0 M OH^-. The proposed mechanism for formation of the hydantoins is a novel metal-assisted intramolecular nucleophilic cyclization reaction. This reaction represents an example of an intramolecular nucleophilic reaction where the nucleophile is a metal-coordinated deprotonated peptide (or amide) nitrogen. Hydantoins are not observed in the photolysis of $Cu^{III}(H_{-2}Aib_3a)^+$ in 4.0 M H^+ since dissociation of the ligand fragments and subsequent hydrolysis is more competitive than intramolecular cyclization.

Acknowledgment. This investigation was supported by an Eastman Kodak Industrial Associates Fellowship (J.P.H.) and by Public Health Service Grant No. GM-12152 from the National Institute of General Medical Sciences. The assistance of Kimber D. Fogelman with the pulsed-accelerated-flow studies is greatly appreciated.

Contribution from the Department of Chemistry,
The University of North Carolina, Chapel Hill, North Carolina 27514

Electrochemistry of *trans*-Dioxo Complexes of Rhenium(V) in Water

David W. Pipes and Thomas J. Meyer*

Received February 20, 1986

Cyclic voltammetry of *trans*-$[(py)_4Re^V(O)_2]^+$ (py is pyridine) in aqueous solutions at glassy-carbon electrodes show that oxidation states Re(VI)(d^1) to Re(II)(d^5) are accessible within the solvent limits. Similar behavior is observed for *trans*-$[(CN)_4Re^V(O)_2]^{3-}$ and *trans*-$[(en)_2Re^V(O)_2]^+$. Reduction of the pyridine complex to Re(II) at $0 \le pH \le 14$ leads to H_2; k_{obsd}(room temp, μ = 0.1 M) = 2.4 ($\pm$1.5) $\times 10^{-3}$ s^{-1} at pH 1.2. At pH 6.8 or 13.0, the addition of NO_2^- or SO_3^{2-} suppresses water reduction at the expense of electrocatalytic reduction of NO_2^- to NH_3 and N_2O and of SO_3^{2-} to H_2S or HS^-. Comparisons between the Re-pyridyl-based couples and the structurally and electronically related *trans*-$[(bpy)_2Os^{VI}(O)_2]^+$ (bpy is 2,2'-bipyridine) couples suggest that the pattern of couples that appear and their pH dependences are determined largely by the d-electronic configurations of the components. Differences in the magnitudes of redox potentials between electronically equivalent Re and Os couples are determined by the differences in oxidation state between the two types of couples.

Introduction

The higher oxidation state oxo complexes of Os and Ru have a rich chemistry as oxidants in reactions as diverse as the oxidation of alcohols to ketones,[1] alllylic C-H groups to carboxylates,[1] phenols to quinones,[2] NO_2^- to NO_3^-,[3] olefins to epoxides,[4] HCO_2^- to CO_2,[5] H_2O to O_2,[6] and Cl^- to Cl_2.[7] The higher oxidation states are stabilized by metal-oxo formation following oxidative deprotonation of aqua or hydroxo groups, e.g.

$$[(bpy)_2(py)Ru^{II}\text{—}OH_2]^{2+} \xrightarrow[-H^+]{-e^-}$$

$$[(bpy)_2(py)Ru^{III}\text{—}OH]^{2+} \xrightarrow[-H^+]{-e^-} [(bpy)_2(py)Ru^{IV}\text{=}O]^{2+}$$ [8a,b]

(bpy is 2,2'-bipyridine; py is pyridine). Stabilization by oxo groups lowers the redox potentials for couples involving higher oxidation states to such a degree that extended series of redox couples are accessible within the solvent limits. For example, potentials for Os(VI/V), Os(V/IV), Os(IV/III), and Os(III/II) couples based on *cis*-$[(bpy)_2Os^{II}(OH_2)_2]^{2+}$ and *cis*-$[(bpy)_2Os^{VI}(O)_2]^{2+}$ occur over a potential range of only 0.7 V at pH 4.[8c,d]

For the Ru and Os complexes as stoichiometric or catalytic oxidants the important feature is the accessibility of higher oxidation state oxo complexes. For Mo, W, and Re in equivalent coordination environments and oxidation states, the metals are more electron-rich and higher oxidation states are the norm as metal-oxo complexes. However, for these metals the possibility exists that, upon reduction and protonation, aqua or hydroxo

(1) (a) Moyer, B. A.; Thompson, M. S.; Meyer, T. J. *J. Am. Chem. Soc.* **1978**, *102*, 2310. (b) Thompson, M. S.; DeGiovani, W. F., Moyer, B. A.; Meyer, T. J. *J. Org. Chem.* **1984**, *25*, 4972.
(2) Roecker, L. Ph.D. Dissertation, The University of North Carolina, Chapel Hill, NC, 1985.
(3) (a) Moyer, B. A.; Meyer, T. J. *J. Am. Chem. Soc.* **1979**, *101*, 1326. (b) McGuire, M., work in progress.
(4) Dobson, J.; Seok, W.; Meyer, T. J. *Inorg. Chem.* **1986**, *25*, 1513.
(5) Roecker, L.; Meyer, T. J. *J. Am. Chem. Soc.*, in press.
(6) (a) Gersten, S. W.; Samuels, G. J.; Meyer, T. J. *J. Am. Chem. Soc.* **1982**, *104*, 4029. (b) Goswanai, S.; Chakravorty, A. R.; Chakravorty, A. *J. Chem. Soc., Chem. Commun.* **1982**, 1288. (c) Gilbert, J. A.; Eggleston, D. S.; Murphy, W. R., Jr.; Geselowitz, D. A.; Gersten, S. W.; Hodgson, D. J.; Meyer, T. J. *J. Am. Chem. Soc.* **1985**, *107*, 3855-3864. (d) Honda, K.; Frank, A. J. *J. Chem. Soc., Chem. Commun.* **1984**, 1436. (e) Collin, J. P.; Sauvage, J. P. *Inorg. Chem.* **1986**, *25*, 135.
(7) (a) Ellis, C. D.; Gilbert, J. A.; Murphy, W. R., Jr.; Meyer, T. J. *J. Am. Chem. Soc.* **1983**, *105*, 4842. (b) Vining, W. J.; Meyer, T. J. *Inorg. Chem.* **1986**, *25*, 2015.
(8) (a) Moyer, B. A.; Meyer, T. J. *Inorg. Chem.* **1981**, *20*, 436. (b) Moyer, B. A.; Meyer, T. J. *J. Am. Chem. Soc.* **1978**, *100*, 3601. (c) Takeuchi, K. J.; Samuels, G. J.; Gersten, S. W.; Gilbert, J. A.; Meyer, T. J. *Inorg. Chem.* **1983**, *22*, 1407. (d) Dobson, J. C.; Takeuchi, K. J.; Pipes, D. W.; Geselowitz, D. A.; Meyer, T. J. *Inorg. Chem.* **1986**, *25*, 2357. (e) Che, C.-M.; Tang, T.-W.; Poon, C. K. *J. Chem. Soc., Chem. Commun.* **1984**, 641.

0020-1669/86/1325-3256$01.50/0